A Differentiable Fast Forward Projector for Multi-pinhole SPECT and Co-registered CT

William Worstell (PicoRad Imaging), Yuemeng Feng, Amirreza Hashemi, Mark Ottensmeyer, Xi Zhang, Hamid Sabet (HMS/Massachusetts General Hospital)

Introduction

Cardiac SPECT (Single Photon Emission Computed Tomography) is a critical imaging modality for diagnosing and managing cardiovascular diseases, providing valuable information on myocardial perfusion and function. Cardiac SPECT/CT, which combines SPECT with computed tomography, offers superior sensitivity and specificity compared to standalone Cardiac SPECT, leading to better patient outcomes (Besson et al., 2024).

We propose a novel differentiable fast forward projector for stationary multi-pinhole SPECT, integrated with co-registered virtual CT. This approach leverages advanced computational techniques to enhance image reconstruction and system calibration, promising significant improvements in diagnostic accuracy and efficiency. Stationary multi-pinhole SPECT is uniquely capable of modeling combined cardiac and respiratory motion, potentially augmented by (or trained with) further X-ray imaging at or near the time of SPECT acquisition (Torkaman et al., 2021; Real-time respiratory triggered SPECT myocardial perfusion imaging using CZT technology, 2020).

We are developing PyTorch-based imaging pipelines for the Dynamic Cardiac SPECT (DC-SPECT) system currently being constructed at the Massachusetts General Hospital, which has 15 times the sensitivity of conventional SPECT systems, and for which this work will help provide DC-SPECT/CT capabilities (Bläckberg et al., 2020; Feng et al., 2023). The diffPose software enables the generation of a virtual CT from a prior patient CT, rigidly or deformably co-registered with the patient's reference CT (Gopalakrishnan et al., 2023). This enables SPECT/CT methods for SPECT-only systems. Motion-corrected models are possible, which can also take advantage of recent advances in generative denoising using stochastic differential equation methods to max- -imize the information content and high spatial-temporal accuracy of neural network models (Wang et al., 2024). diffPose uses recent releases of diffDRR which support point clouds as well as voxels, plus both direct and inverse projection transforms using homogeneous coordinates, fast coordinate transformations, fast matrix multiplications, and neural networks.

Figure 2 illustrates diffPose function, with diffDRR driving its parallel software implementation. diffDRR utilizes PyTorch, which offers a simpler development process with equally fast execution in comparison with C++ and CUDA development. diffDRR vectorizes the Siddon method for efficient and accurate ray-tracing in digitally reconstructed radiographs, enhancing the performance and scalability of deep learning-based imaging pipelines (Gopalakrishnan & Golland, 2022).

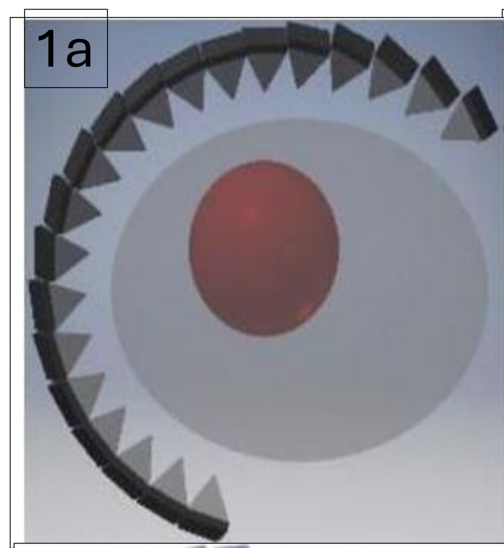

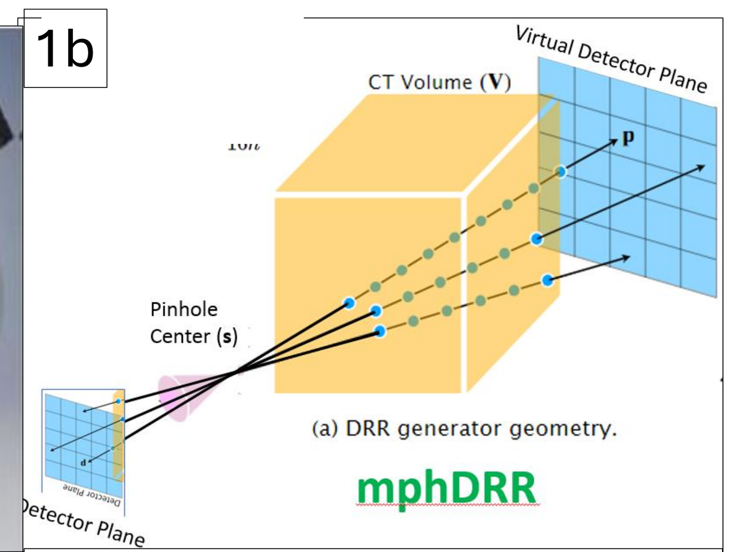

Figure 1a: GATE model of DC-SPECT, a stationary dynamic cardiac SPECT system, with 80 detector modules focally arranged (Bläckberg). This geometry yields 15x more sensitivity at comparable resolution to conventional dual head gamma cameras.

Figure 1b: diffDRR parallel implementation of ray-tracing and line integral summation using the Siddon method and our Geometry.

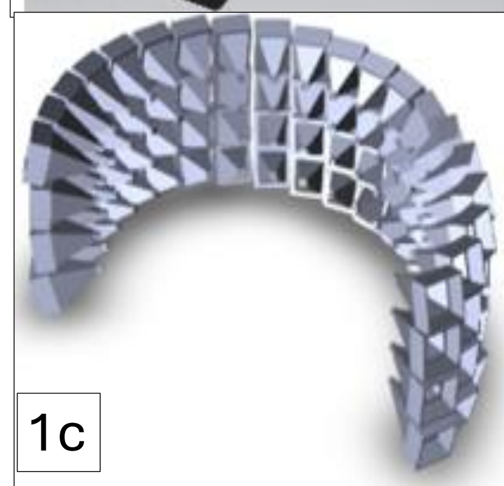

Figure 1c: DC-SPECT system 3D geometry CAD display, illustrating the focal alignment of all the modules' principal rays.

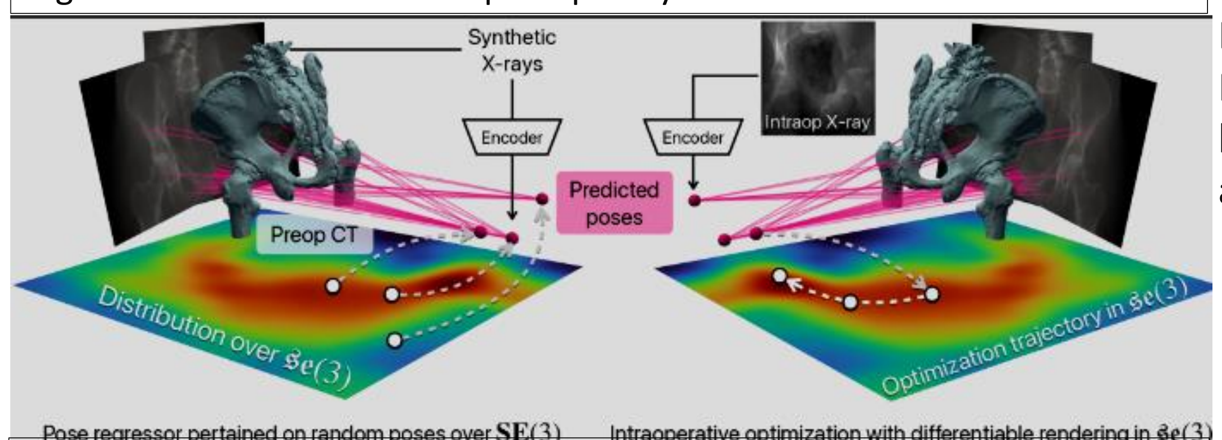

Figure 2: diffPose: An intraoperative system leveraging deep learning to align rapid 2D intraoperative images, such as X-rays, with high-fidelity 3D preoperative reference CT scans, enhancing surgical precision and accuracy. (from Gopalakrishnan, 2023)

Methods

We build upon the diffDRR open-source software from the MIT CSAIL Lab (Gopalakrishnan & Golland, 2022) to provide differentiable SPECT forward projection rendering and optimization in PyTorch for the Dynamic Cardiac SPECT (DC-SPECT) system under development at the Massachusetts General Hospital. The system, currently being commissioned, features a wide focal field of view (FOV) optimized for cardiac imaging (15 cm diameter) as shown in Fig 1 and described in【4】and【5】. The multi-pinhole stationary SPECT geometry is related by a 3D inversion through each pinhole center to a corresponding array of pinhole cameras. With slight modifications, diffDRR can efficiently and differentiably generate SPECT 3D forward projections and co-registered virtual CT images of the subject being imaged.

We incorporate the diffPose framework, also from MIT CSAIL, which facilitates intraoperative 2D/3D registration using differentiable X-ray rendering (Gopalakrishnan et al., 2023). This technique enables co-registration of virtual CT images using C-arm images acquired at or near contemporaneously with SPECT data. Eliminating a dedicated CT system yields cost savings and system design benefits. Our application of diffDRR to the DC-SPECT system was implemented using JuPyter notebooks on Google Colab, with code and documentation available on GitHub.

Using diffDRR, we project CT volumes through synthetic C-arm projection images, allowing visualization of each camera's FOV and the surrounding context. This is particularly useful for developing high-resolution displays showing the multipinhole SPECT camera's FOV across the CT volume. The forward projection rendering uses Siddon's method, and diffDRR has been optimized for GPU-accelerated tensor computation to achieve rendering speeds equivalent to state-of-the-art DRR generators implemented in CUDA and C++.

In our setup, we specified the DC-SPECT system geometry in an Excel spreadsheet and interfaced with it using the OpenPyXL package. We then called diffDRR repeatedly, cycling through the 80 camera poses to build up a forward-projected, multiple perspective projection 3D data tensor for a given input source volume. We then evaluated the forward projection of the diffDRR standard CT test volume visually to check the FOV for our DC-SPECT system, as shown in Figure 3.

For future work, we aim to include attenuation correction and sensitivity modeling by modifying the line integral kernels, and accounting for attenuation effects (using mass density and electron density volumes from spectral CT images) by scaling attenuation effects to SPECT gamma-ray energies. This will help to improve image and quantitative accuracy of DC-SPECT cardiac images.

Results

- The forward projection of the diffDRR standard CT test volume was visually evaluated to check the field view for our DC-SPECT system.
- The diffDRR projections from the DC-SPECT camera show evident 3D parallax image information at high spatial resolution in the depth-of-field.
- Examination of field-of-view effects given the focal geometry of the DC-SPECT system shows the importance of patient positioning for optimal imaging, with or without auxiliary imaging at or near DC-SPECT imaging time by another modality such as C-Arm X-ray.
- Version 0.4 of diffDRR required 17.7 seconds running on a Google Colab L4 GPU (versus 230 seconds on CPU) to generate 80 projections, each a 250 x 250 pixel DRR from a CT test volume of [512, 512, 133] with [0.7, 0.7, 2.5] mm spacing.
- The diffDRR projections from the DC-SPECT within various camera poses in Extra wide FOV indicate potential sources of limited-angle and out-of-field source and attenuation contributions that need to be included.
- A Jupyter notebook detailing all required steps to generate Figure 4 below is posted, open source, at https://github.com/PicoRad-Imaging/SNM2024 as SNMMI2024.ipynb.

Conclusion

diffDRR is a powerful tool for developing Deep Learning Imaging Pipelines for the DC-SPECT and its DC-SPECT/VirtualCT Extension. Using parallax between axially and transaxially adjacent cameras, depth information along the projection axis can be fed into 3D image reconstruction pipelines. The DiffDRR projections from the DC-SPECT camera poses with expanded fields of view indicate that for both emission images and their attenuation correction an extension to a wide FOV to capture the entire CT volume is needed. DiffDRR uses rapid parallel implementation of Einstein summation for tensors, which can be unrolled into iterative image reconstruction pipelines. Deep learning methods developed for Limited-Angle and Sparse-Angle CT can be applied to SPECT by forming a factorized System Matrix, convolving with a Detector response function informed by measured or learned modulation transfer functions. Sampling at high spatial frequencies, as in the [80,250,250] projection tensors shown here, can then address partial volume effects in source and attenuation distributions with uniform temporal sampling at super-resolution for SPECT in hybrid DC-SPECT/VirtualCT imaging.

The authors acknowledge financial support of the NIH Grant No. R01HL145160

References

1. Besson, F.L., Treglia, G., Bucerius, J., Anagnostopoulos, C., Buechel, R.R., Dweck, M.R., Erba, P.A., Gaemperli, O., Gimelli, A., Gheysens, O., & Glaudemans, A.W. (2024). A systematic review for the evidence of recommendations and guidelines in hybrid nuclear cardiovascular imaging. European Journal of Nuclear Medicine and Molecular Imaging, pp.1-13.
2. Torkaman, M., Yang, J., Shi, L., Wang, R., Miller, E.J., Sinusas, A.J., Liu, C., Gullberg, G.T., & Seo, Y. (2021, February). Direct image-based attenuation correction using conditional generative adversarial network for SPECT myocardial perfusion imaging. In Medical Imaging 2021: Biomedical Applications in Molecular, Structural, and Functional Imaging (Vol. 11600, pp. 203-211). SPIE.
3. Real-time respiratory triggered SPECT myocardial perfusion imaging using CZT technology. (2020). European Heart Journal - Cardiovascular Imaging. Available at: https://academic.oup.com/ehjci/article/22/1/69/5644291.
4. Bläckberg, L., et al. (2020). Dynamic Cardiac SPECT for diagnostic and theranostics applications: latest results. In 2020 IEEE Nuclear Science Symposium and Medical Imaging Conference (NSS/MIC) (pp. 1-3). IEEE.
5. Feng, Y., Worstell, W., Kupinski, M., Furenlid, L.R., Sabet, H. (2023). Resolution recovery on list mode MLEM reconstruction for Dynamic Cardiac SPECT system. arXiv preprint arXiv:2212.14505.
6. Gopalakrishnan, V., Dey, N., & Golland, P. (2023). Intraoperative 2D/3D Image Registration via Differentiable X-ray Rendering. arXiv preprint arXiv:2312.06358.
7. Gopalakrishnan, V., & Golland, P. (2022). Fast auto-differentiable digitally reconstructed radiographs for solving inverse problems in intraoperative imaging. In Workshop on Clinical Image-Based Procedures (pp. 1-11). Cham: Springer Nature Switzerland.
8. Wang, Y., Yoon, S., Jin, P., Tivnan, M., Chen, Z., Hu, R., Zhang, L., Chen, Z., Li, Q., & Wu, D. (2024). Implicit Image-to-Image Schrodinger Bridge for CT Super-Resolution and Denoising. arXiv preprint arXiv:2403.06069.

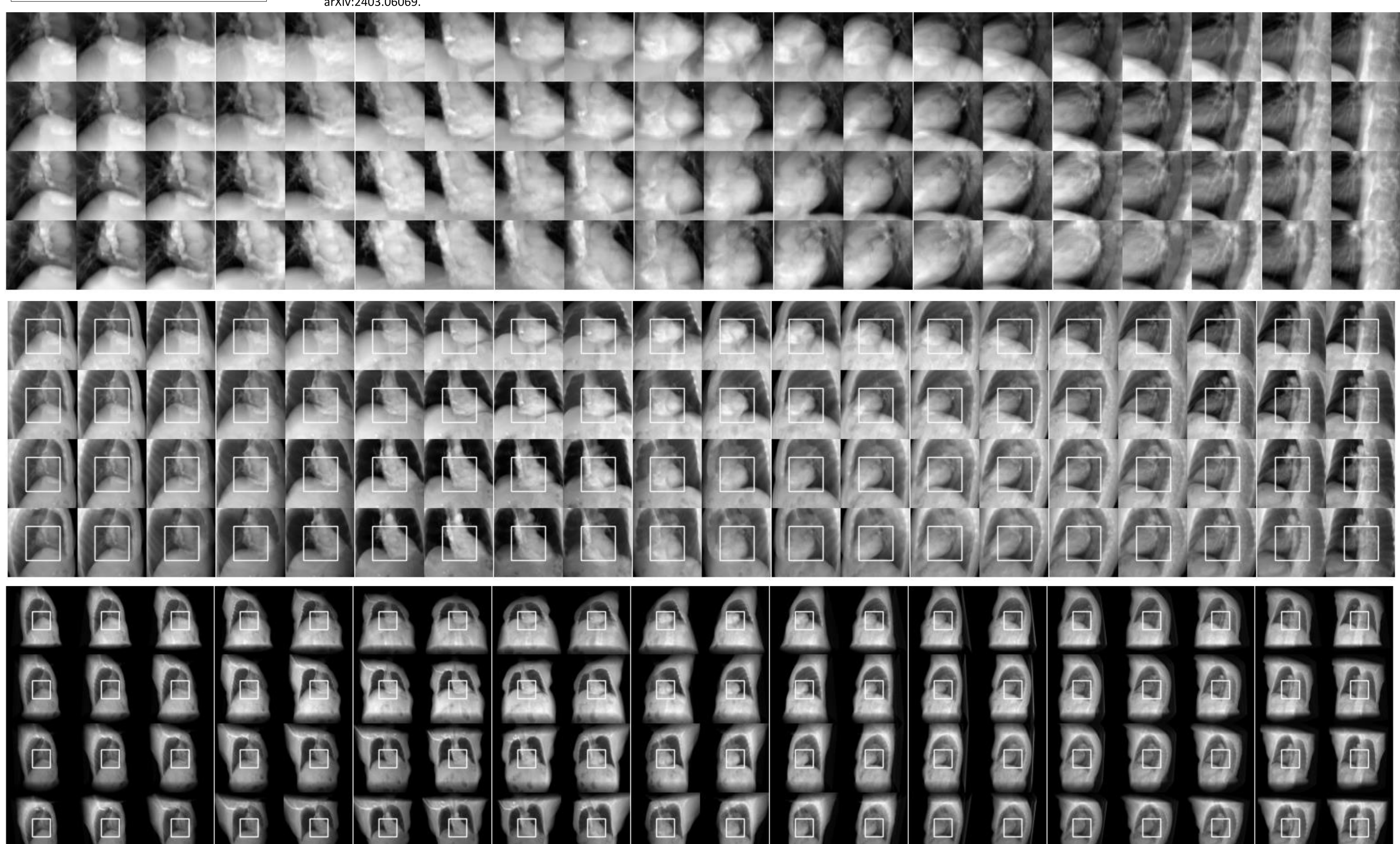

Figure 3: FOV, Wide FOV, and Extrawide FOV: Demonstrates the capability of the DC-SPECT system for quantitative SPECT/CT imaging. The DC-SPECT FOV is shown at the top, the Wide FOV in the center highlights the DC-SPECT FOV within it outlined with a white rectangle, and the Extrawide FOV at the bottom again shows the DC-SPECT FOV outlined in white. The system accounts for source and attenuator tissues within the FOV of one camera but outside the FOV of others, enhancing diagnostic accuracy and enabling comprehensive image analysis.